HHS Public Access

Author manuscript

J Comp Neurol. Author manuscript; available in PMC 2018 January 09.

Published in final edited form as:

J Comp Neurol. 2015 December 01; 523(17): 2477–2494. doi:10.1002/cne.23848.

Degeneration of Proprioceptive Sensory Nerve Endings in Mice Harboring Amyotrophic Lateral Sclerosis–Causing Mutations

Sydney K. Vaughan[1,4], **Zachary Kemp**[1], **Theo Hatzipetros**[2], **Fernando Vieira**[2], and **Gregorio Valdez**[1,3,*]

[1]Virginia Tech Carilion Research Institute, Virginia Tech, Roanoke, Virginia, USA

[2]ALS Therapy Development Institute, Cambridge, Massachusetts 02139

[3]Department of Biological Sciences, Virginia Tech, Blacksburg, Virginia 24061

[4]Graduate Program in Translational Biology, Medicine, and Health, Virginia Tech, Blacksburg, Virginia, USA

Abstract

Amyotrophic lateral sclerosis (ALS) is a neurodegenerative disease that primarily targets the motor system. Although much is known about the effects of ALS on motor neurons and glial cells, little is known about its effect on proprioceptive sensory neurons. This study examines proprioceptive sensory neurons in mice harboring mutations associated with ALS, in SOD1^{G93A} and TDP43^{A315T} transgenic mice. In both transgenic lines, we found fewer proprioceptive sensory neurons containing fluorescently tagged cholera toxin in their soma five days after injecting this retrograde tracer into the tibialis anterior muscle. We asked whether this is due to neuronal loss or selective degeneration of peripheral nerve endings. We found no difference in the total number and size of proprioceptive sensory neuron soma between symptomatic SOD1^{G93A} and control mice. However, analysis of proprioceptive nerve endings in muscles revealed early and significant alterations at Ia/II proprioceptive nerve endings in muscle spindles before the symptomatic phase of the disease. Although these changes occur alongside those at α-motor axons in SOD1^{G93A} mice, Ia/II sensory nerve endings degenerate in the absence of obvious alterations in α-motor axons in TDP43^{A315T} transgenic mice. We next asked whether proprioceptive nerve endings are similarly affected in the spinal cord and found that nerve endings terminating on α-motor neurons are affected during the symptomatic phase and after peripheral nerve endings begin to degenerate. Overall, we show that Ia/II proprioceptive sensory neurons are affected by ALS-causing mutations, with pathological changes starting at their peripheral nerve endings.

INDEXING TERMS

Amyotrophic Lateral Sclerosis (ALS); SOD1^{g93A}; TDP43^{A315T}; Proprioceptive sensory neuron; Motor neuron; Neuromuscular junction (NMJ); VAChT; VGLUT1

*CORRESPONDENCE TO: Gregorio Valdez, Virginia Tech Carilion Research Institute, Virginia Tech, 2 Riverside Circle, Roanoke, VA 24016. gvaldez1@vtc.vt.edu.

CONFLICT OF INTEREST STATEMENT

The authors have no conflict of interest to declare.

Amyotrophic lateral sclerosis (ALS) is an adult-onset neurodegenerative disease characterized by degeneration of motor axons and atrophy of skeletal muscle fibers. Once symptoms arise, the disease progresses rapidly, and 80% of patients die within five years of diagnosis from respiratory failure (Hardiman et al., 2011). Because the disease ravages the motor system, ALS was believed only to affect motor neurons. However, it has recently become clear that ALS is a multisystem disorder, largely because of the discovery of mutant genes that cause the disease (Pugdahl et al., 2007; Ng et al., 2015). For example, individuals with mutations in the 43-kDa TAR DNA binding protein (TDP-43) and RNA-binding protein FUS/TLS (FUS) are afflicted with both ALS and frontotemporal dementia (Neumann et al., 2006; Ling et al., 2013). Thus, we now know that the disease affects a variety of cells, including glial and Renshaw cells in the spinal cord (Boillée et al., 2006a; Haidet-Phillips et al., 2011; Mochizuki et al., 2011; Ozdinler et al., 2011; Wootz et al., 2013; Philips and Rothstein, 2014). Many of these cells in fact contribute to ALS-associated pathogenesis and in large part by affecting the susceptibility of α-motor neurons to the disease (Boillée et al., 2006b; Jaarsma et al., 2008; Mead et al., 2011).

There is growing evidence that sensory neurons are also affected in ALS. In humans, neuroimaging and neurophysiological tests have detected abnormalities in 20–60% of sensory neurons in patients afflicted with ALS (Hammad et al., 2007; Pugdahl et al., 2007; Pradat and El Mendili, 2014), and histological analyses have revealed degeneration of these neurons and their axons (Dyck et al., 1975; Hanyu et al., 1982; Bradley et al., 1983; Hammad et al., 2007). Similar pathological changes in sensory neurons have been observed in mouse models of the disease (Guo et al., 2009; Hatzipetros et al., 2014; Sábado et al., 2014). Although we know that sensory neurons exhibit pathological features in symptomatic $SOD1^{G93A}$ mice, these alterations could be the result of degeneration in other cells and wasting of the animal as it approaches death.

Among sensory neurons, degeneration of proprioceptive sensory neurons, particularly Ia/II proprioceptors, would arguably have the greatest impact on α-motor neurons and ALS-related motor decline. These pseudounipolar neurons are located in dorsal root ganglia (DRG), from which they send axonal branches to skeletal muscles and to the spinal cord. Proprioceptive peripheral nerve endings innervate muscle spindles (Ia/II afferents) and Golgi tendon organs (Ib afferents) to detect changes in muscle length, velocity, and tension. Ia/II Afferents directly transmit these changes to α-motor neurons via monosynaptic connections. Thus, Ia/II proprioceptive sensory and α-motor neurons are functionally and structurally connected. Underscoring the importance of this relationship, loss of proprioceptive inputs exacerbates α-motor neuron dysfunction in spinal muscular atrophy (Mentis et al., 2011).

Here, we examine proprioceptive sensory neurons in two transgenic mouse lines harboring ALS-causing mutant human genes, $SOD1^{G93A}$ and $TDP43^{A315T}$ (Gurney et al., 1994; Wegorzewska et al., 2009). We demonstrate that Ia/II proprioceptive peripheral nerve endings degenerate before the appearance of neurological symptoms and loss of centrally projecting nerve branches. These nerve endings follow a similar time course and pattern of degeneration as α-motor neurons in $SOD1^{G93A}$ transgenic mice. In contrast, Ib proprioceptive sensory and γ-motor nerve endings are mostly spared at all ages examined. Overall, the data presented in this article strongly suggest that peripheral nerve endings are

the focal sites of pathology in Ia/II proprioceptive sensory neurons and α-motor neurons in two mouse models of ALS.

MATERIALS AND METHODS

Source of mice

The following mice were obtained from Jackson laboratories: $SOD1^{G93A}$ (Gurney et al., 1994), parvalbumin-Cre (referred to here as *PVCre*; Hippenmeyer et al., 2005), and Thy1-STOP-YFP line 15 (referred to here as *STP-YFP*; Buffelli et al., 2003). $TDP43^{A315T}$ mice (Wegorzewska et al., 2009) were obtained from ALS TDI via Charles River, and Thy1-YFP16 (referred to here as *Thy1-YFP*; Feng et al., 2000) mice were a generous gift from Dr. Joshua R. Sanes. To visualize motor and sensory axons in the same muscle, we generated mice expressing Thy1-YFP16 and $SOD1^{G93A}$ (referred to as *Thy1-YFP;SOD1*^{G93A}). To visualize proprioceptive sensory axons exclusively, we mated PVCre and STP-YFP (referred to as *PVCre;STP-YFP;SOD1*^{G93A}). Only male mice were used for structural analysis of nerve endings and to examine sensory soma. Mice were anesthetized with isoflurane and then perfused transcardially first with 10 ml of 0.1 M PBS, followed by 25 ml of 4% paraformaldehyde in 0.1 M PBS (pH 7.4). All experiments were carried out under NIH guidelines and animal protocols approved by the Virginia Tech Institutional Animal Care and Use Committee.

Antibody characterization

All antibodies used in this study are routinely used to label axons and nerve endings in the spinal cord and muscles by immunohistochemistry (IHC). Table 1 contains information for each antibody used, including their original source.

Synaptotagmin-2 (Syt2)—The antibody against synaptotagmin-2 (Syt2), also called *ZNP1* (Trevarrow et al., 1990), recognizes mouse Syt2 by Western blot and IHC analysis (Fox and Sanes, 2007). It detects a 60-kDa band that corresponds to Syt2. It also selectively labels the presynaptic nerve endings of sensory and motor neurons in muscles (Valdez et al., 2012) and synaptic sites in the brain (Cooper and Gillespie, 2011).

Synaptophysin—The synaptophysin antibody was designed to detect the C-terminus of human synaptophysin. It specifically labels presynaptic terminals. However, the antibody also recognizes mouse synaptophysin and axonal nerve endings known to express this molecule (Lai et al., 2008; Harrington et al., 2012).

Neurofilament (SMI-312)—SMI-312 is a cocktail of antiphospho-neurofilament antibodies (SMI-312R) and detects a 200–220-kDa band by Western blot analysis. It has been well characterized as a marker of peripheral axons, including sensory and motor axons (Sternberger et al., 1982), as well as axons in the central nervous system (Petralia et al., 2011).

VAChT—VAChT antibody against the vesicular acetylcholine transporter detects a 57-kDa protein. On IHC, the distribution of this protein matches the ditributions previously reported

for the spinal cord and motor neurons somata (Duplan et al., 2010; Enjin et al., 2010; Wootz et al., 2013).

VGluT1—VGluT1 antibody against vesicular glutamate transporter 1 detects a 45–55-kDa protein (Garbelli et al., 2008). The IHC pattern for VGluT1 in the spinal cord matches the reported distribution of this protein (Balaram et al., 2015).

NeuN—The NeuN antibody detects a neuron-specific protein localized in the nucleus with a molecular weight of 46–48 kDa (Mullen et al., 1992). In our hands, this antibody labels only neuronal nuclei in the spinal cord and DRGs, in accordance with previous findings (Scott and Lois, 2007).

Muscle IHC

Whole extensor digitorum longus (EDL) muscles were used to visualize sensory and motor nerve endings and their targets. To analyze motor and sensory nerve endings in the same muscle, $SOD1^{G93A}$ and control animals expressing YFP (Thy1-YFP) in all neurons were used. To visualize the soma, control and $SOD1^{G93A}$ mice expressing YFP exclusively in proprioceptive sensory neurons were used. Nerve endings in $TDP43^{A315T}$ were visualized with antibodies. Muscles were blocked for at least 1 hour at room temperature with 0.1% Triton X-100, 4% BSA, and 5% goat serum in 1× PBS. Muscles were then incubated with antibodies to neurofilaments (smi-312; Covance, Berkeley, CA; 1:1000), synaptophysin (Invitrogen, Carlsbad, CA; 1:100) and synaptotagmin-2 (znp-1; Zebrafish International Resource Center; 1:250) for at least 24 hours in blocking solution. Muscles were washed three times with 1× PBS and incubated for at least 24 hours with secondary antibodies (Alexa-488 or Alexa-568 anti-mouse IgG2a and Alexa-647 anti-mouse IgG1; Molecular Probes, Eugene, OR). All muscles were also incubated with Alexa-555-tagged bungarotoxin (Life Technologies, Grand Island, NY; 1:1,000) diluted in blocking buffer together with secondary antibodies or in 1× PBS for at least 1 hour to visualize nicotinic acetylcholine receptor (AChR) clusters. After being washed three times with 1× PBS, muscles were mounted with Vectashield (Vector, Burlingame, CA).

Spinal cord IHC

Spinal columns were dissected immediately after perfusion and postfixed in 4% paraformaldehyde (PFA) overnight at 4°C. After postfixation, the spinal column was washed three times with 1× PBS and then cut in half at the last rib to separate the lumbar and sacral regions from the thoracic and cervical regions. The different regions of the spinal cord were isolated and placed in 30% sucrose overnight at 4°C. The spinal cord segments were then placed in a Fisherbrand base mold with Tissue Freezing Medium from Triangle Biomedical Sciences, Inc. With a cryostat, 20-μm sections were collected on gelatin-coated slides. After being washed three times with 1× PBS, the sections were blocked for 1 hour with 0.05% Triton X-100, 4% BSA, and 5% goat serum diluted in 1× PBS. After incubation with primary antibodies overnight at 4°C, the slides were washed three times with 1× PBS and incubated with secondary antibodies at room temperature for 2 hours. The sections were washed an additional three times with 1× PBS, incubated with DAPI (1:1,000) for 5 minutes, and mounted. The following primary antibodies diluted in blocking buffer were

used to label spinal cord sections: vesicular acetylcholine transporter (VAChT; Millipore. Bedford, MA; 1:250), vesicular glutamate transporter (VGluT1; Synaptic Systems; 1:250), and NeuN (Millipore; 1:250). We used the following secondary antibodies from Life Technologies diluted 1:1,000 in blocking buffer: Alexa-555 goat anti-guinea pig, Alexa-647 goat anti-rabbit, and Alexa-488 goat anti-mouse IgG1. Prior to mounting, sections were also stained with DAPI (4′,6-dia-midino-2-phenylindole: Sigma, St. Louis, MO; 1:1,000) to reveal nuclei.

Cholera toxin subunit B injections and visualization of proprioceptive sensory soma

The tibialis anterior muscle of PvCre;STP-YFP animals was injected with 2.5 μl of 0.25 mg/ml Alexa-555-conjugated cholera toxin subunit B (fCTB; Molecular Probes, Eugene, OR) one time and into the belly of the muscle. In another experiment, we injected 25 μl of fCTB into multiple locations of the muscle. Five days postinjection, mice were perfused and intact DRGs isolated. After removing the outer membrane, DRGs expressing YFP in proprioceptive sensory neurons were whole mounted. For $TDP43^{A315T}$ and control animals not expressing YFP, DRGs were placed in 96 wells, blocked, and incubated with antibodies following the same protocol described above to stain nerve endings in muscles. To visualize whole DRGs and examine sensory soma, high-resolution images were taken and tiled with a Zeiss LSM 700 motorized confocal microscope. The number of fCTB-positive neurons, soma size and the number of neurons expressing YFP in the same DRG were quantified in ImageJ.

Analysis of nerve endings in muscles and spinal cords

Peripheral nerve endings—To analyze proprioceptive nerve endings and neuromuscular junction (NMJ) structures, maximum intensity projections from confocal stacks were created with Zen Black (Zeiss). The following structural features were compared between groups: 1) distance between spirals; in ImageJ software, the distance in micrometers was measured between each annulospiral wrapping around the belly of the muscle spindle; 2) unravelling (lack of annulospirals or significantly disorganized annulospirals at the equatorial region of intrafusal muscle fibers); and 3) innervation of AChR clusters, defined as colocalization of axon terminals, labeled with YFP or synaptotagmin-2 and neurofilament, with fluorescently labeled AChRs. γ-Motor nerve endings were identified based on their innervation of AChR clusters located at the equatorial region of intrafusal muscle fibers. α-Motor nerve endings exclusively innervate AChR clusters on extrafusal muscle fibers (NMJ), and these clusters are larger and structurally more complex than those on intrafusal muscle fibers, making it easy to distinguish the two types. ALS-related changes at NMJs were scored based on the definitions described by Valdez et al. (2012). In all these experiments, at least six animals per age group and 100 NMJs per animal were examined. A Student *t*-test with $P < 0.05$ was used to determine significance.

Axon number—To determine whether degeneration of nerve endings results in loss of sensory axons, we determined the number of sensory and α-motor axon in the EDL muscle of $SOD1^{G93A}$ and control mice expressing YFP in sensory and motor axons. The EDL muscle can be separated into four smaller muscles by pulling on the tendons that attach the muscle to the four smaller toes. We counted motor and sensory axons innervating the

outermost portion of the EDL, which attaches to the fifth toe. Both types of axons can be easily identified soon after the nerve enters the muscle and branches to innervate different regions of the endplate band, spindles, and Golgi tendons. We counted sensory axons by tracing all axons innervating spindles and Golgi tendons. α-Motor axons were counted by tracing back the nerve branch that innervates the most distal NMJs in the outermost division of the EDL muscle, as depicted in Figure 3.

Glutamatergic and cholinergic synapses on motor soma—High-resolution confocal images were obtained exclusively from the ventral horn of the spinal cord. VGluT1-and VAChT-positive puncta adjacent to the peripheral membrane of α-motor neuron soma, labeled with YFP or NeuN, were counted in ImageJ. The perimeter of the same α-motor neuron soma was determined to assess the ratio of synaptic puncta to soma size. At least 10 neurons per mouse and three mice per group were used for this analysis.

RESULTS

Analysis of proprioceptive sensory neurons innervating ALS-affected muscles

We first examined proprioceptive sensory neurons in SOD1^{G93A} transgenic mice. We focused on proprioceptive sensory neurons for the following reasons: their close anatomical and functional relationship with α-motor neurons and thus critical function in the motor system; the soma and nerve endings being relatively easy to analyze compared with other sensory neurons; and, because their peripheral nerve endings innervate skeletal muscles, the ability to compare alterations to those in α-motor axons directly. To facilitate analysis of proprioceptive sensory neurons and their nerve endings, we crossed parvalbumin-Cre (PVCre; Hippenmeyer et al., 2005) and Thy1-STOP-YFP (STP-YFP; Buffelli et al., 2003) mice to generate mice expressing YFP selectively in parvalbumin-positive cells (PVCre;STP-YFP; Fig. 1A). In DRGs, the parvalbumin promoter is active only in proprioceptive sensory neurons. Hence, Cre recombinase expression results in the excision of the STOP cassette, allowing YFP to be selectively expressed and mark these neurons (Fig. 1B–D). We examined proprioceptive sensory neurons innervating the tibialis anterior (TA) muscles because hind limb muscles are severely affected in SOD1^{G93A} mice.

To determine the number and location of proprioceptive sensory neurons innervating the TA muscle, we focally injected 2.5 μl of fCTB (0.25 mg/ml), a retrograde tracer, into the belly of this muscle group. Five days post-injection, we found sensory neurons labeled with fCTB in lumbar regions L2–4 DRGs, with the majority located in L3 DRGs (Fig. 1B–D). We thus focused our analysis on sensory neurons located in L3 DRGs. In control and SOD1^{G93A} mice, proprioceptive sensory neurons were relatively easy to identify by their selective expression of YFP in addition to their large soma (Fig. 1B–D). In comparison with control mice of the same age and sex, we found a significant decrease in the number of fCTB-positive proprioceptive sensory neurons in 90-day-old SOD1^{G93A} transgenic mice (Fig. 1C,E; 9 ± fCTB-positive neurons in ctrl, 2.5 ± 0.7 in SOD1^{G93A}; $P = 7.0 \times 10^{-8}$); this is an age at which these animals begin to exhibit neurological symptoms.

Because we identified proprioceptive sensory neurons after focally injecting a small volume of fCTB, we were concerned that only a few nerve endings were exposed to fCTB. This was

a greater possibility in ALS mice, in which changes in the extracellular matrix and fat deposits from atrophying muscle fibers could impede the diffusion of fCTB. To ensure that all proprioceptive neurons in control and SOD1^{G93A} mice had an equal chance of taking up fCTB, we injected a larger volume of fCTB and into multiple locations in the TA muscle. Using this approach, we again found significantly fewer proprioceptive sensory neurons containing fCTB in SOD1^{G93A} compared with control mice in L3 DRGs (Fig. 1F; 31 ± 3.9 fCTB neurons in ctrl, 5.5 ± 2.3 in SOD1^{G93A}; $P = 0.02$). In all these experiments, we found YFP-negative neurons labeled with fCTB in L3 DRGs. However, their reduced soma size (McMahon et al., 1994) suggest that they are nociceptive and mechanoreceptive sensory neurons (Fig. 2A,B,D,E).

We next asked whether there is a similar reduction of fCTB-positive proprioceptive sensory neurons in TDP43^{A315T} transgenic mice. In published data, these animals were found to contain fewer sensory axons in the femoral nerve branch at 3 and 5 months of age (Hatzipetros et al., 2014). We examined proprioceptive sensory neurons in L3 DRGs from 90-day-old male TDP43^{A315T} transgenic mice after focally injecting 2.5 μl of fCTB into the TA muscle. We again found a significant decrease in the number of fCTB-positive proprioceptive sensory neurons in TDP43^{A315T} transgenic compared with control mice (Fig. 1E; 9 ± 1.41 fCTB-positive neurons in ctrl, and 5 ± 1.2 in TDP43^{A315T}; $P = 0.05$). Together, these data suggested that proprioceptive sensory neurons are affected in two transgenic mouse lines harboring ALS-causing mutant genes.

The number and size of sensory soma are unchanged in early symptomatic SOD1^{G93A} mice

The findings that fewer proprioceptive sensory soma contain fCTB in ALS-affected mice could be due to neuronal loss, selective degeneration of peripheral nerve endings, or inability to take up and retrogradely transport fCTB. We first asked whether proprioceptive sensory neurons degenerate in early symptomatic SOD1^{G93A} mice. Using mice expressing YFP selectively in proprioceptive sensory neurons, we determined their number in L3 DRGs of 90-day-old control and SOD1^{G93A} mice (PVCre;STP-YFP;SOD1^{G93A}). For control mice, we found 544 ± 15.5 sensory neurons expressing YFP (Fig. 1G), representing a minority of all sensory neurons in L3 DRGs, which have been reported to range from 4,000 to 6,000 (Lawson, 1979; McMahon et al., 1994). We found a similar number of propriocepitve sensory neurons in SOD1^{G93A} as in control mice (Fig. 1G; 519 ± 31.6 in SOD1^{G93A} vs. 544 ± 15.5 in ctrl). To determine whether these and other sensory neurons were in the process of degenerating, we measured the size of all sensory neurons soma labeled with fCTB. As expected, YFP positive neurons (1,000–2,000 μm^2) were consistently larger than YFP-negative neurons (medium diameter 600–900 μm^2 and small diameter 200–500 μm^2) in control and SOD1^{G93A} mice (Fig. 2A–F). However, we found no difference in soma size between SOD1^{G93A} and control mice among the three different sensory subgroups (Fig. 2D–F).

Degeneration of peripheral proprioceptive nerve endings in SOD1^{G93A} and TDP43^{A315T} mice

We next probed the possibility that ALS causes degeneration of proprioceptive peripheral nerve endings at muscle spindles, thus explaining the lack of fCTB uptake from the TA muscle. To visualize all sensory and motor nerve endings in muscles, we used mice expressing YFP in all neurons (Thy1-YFP line 16 [Feng et al., 2000]; referred to as Thy1-YFP). We examined sensory nerve endings in the EDL muscle, which is adjacent to the TA muscle and similarly affected by ALS-causing mutations in mice. Unlike the TA and other hind limb muscles, however, the EDL muscle can be separated into four smaller divisions by pulling on their tendons, each attaching to a specific toe. We examined the three smaller divisions of the EDL muscle because they are small enough in adult mice to be whole mounted. This makes it possible to count innervating sensory and motor axons (Fig. 3A) in the same muscle used to examine the structural integrity of their nerve endings (Fig. 3B,C) via light microscopy. For control mice, we found approximately seven muscle spindle units, each containing on average two annulospirals and one flower-spray type proprioceptive sensory nerve ending that wraps around the equatorial region of intrafusal muscle fibers (Fig. 4A) in these three divisions of the EDL. The number and structure of these afferents were similar in control animals from 60 to 120 days of age (Fig. 4A,C). To determine whether these nerve endings were affected in ALS, we examined their structural integrity in presymptomatic (60 days old) and symptomatic (90 days old) SOD1^{G93A};Thy1-YFP mice. We found early and significant structural alterations before the appearance of obvious neurological symptoms (Fig. 4B,C). At 60 days of age, the distance between spirals became highly irregular in SOD1^{G93A};Thy1-YFP mice (Fig. 4B,C). As the disease progressed, Ia/II nerve endings unraveled from muscle spindles and completely degenerated (Fig. 4D).

We explored the possibility that Ia/II proprioceptive neurons are also affected in 90-day-old TDP43^{A315T} mice. For this analysis, we used antibodies against neurofilament and synaptophysin to visualize axons and their nerve endings, respectively. As in SOD1^{G93A} mice, we found obvious structural changes at sensory nerve endings in TDP43^{A315T} mice. In particular, annulospiral endings were found unwinding from intrafusal muscle fibers (Fig. 4D). Thus, Ia/II proprioceptive peripheral nerve endings undergo significant structural alterations in two mouse models for ALS. These findings strongly suggest that degeneration of peripheral nerve endings accounts for the reduced number of proprioceptive sensory neurons positive for fCTB. However, this analysis does not preclude the possibility that retrograde transport deficits contribute to the reduced number of neurons labeled with fCTB.

Proprioceptive nerve endings degenerate independently of α-motor axons

A hallmark of ALS is early retraction of α-motor axons from NMJs (Rocha et al., 2013; Moloney et al., 2014), the synapse formed with extrafusal skeletal muscle fibers. We thus sought to determine whether changes at Ia/II proprioceptive and α-motor peripheral nerve endings occur together or independently. We examined α-motor nerve endings at NMJs in the same EDL muscles used to assess the integrity of Ia/II sensory nerve endings in 90-day-old SOD1^{G93A} (Fig. 3B,C) and TDP43^{A315T} mice. In these muscles, α-motor axons were also marked with YFP (control and SOD1^{G93A}) or neurofilament and synaptophysin (control and TDP43^{A315T}). Postsynaptic sites on extrafusal muscle fibers were labeled with

fluorescently tagged α-bungarotoxin (fBTX), a toxin that binds selectively and with high affinity to muscle nicotinic acetylcholine receptors (AChRs). As previously shown in 90-day-old SOD1^{G93A} mice, α-motor axons are found disconnecting from muscle fibers (percentages denervated: 0 in ctrl, 42 in SOD1^{G93A}; percentages partial innervation: 2 in ctrl, 30 in SOD1^{G93A}; percentages fully innervated: 98 in ctrl, 28 in SOD1^{G93A}), with many NMJs partially or completely denervated compared with those of control mice (Fig. 5A,B,E). Along with these alterations at NMJs, we found fewer α-motor axons in the EDL muscle, and this reduction was similar to that observed for proprioceptive sensory axons in the same muscle (Fig. 4E; 23% motor vs. 19% sensory). Motor and sensory axons were counted by tracing nerve branches, as shown in Figure 3A, innervating the EDL division that attaches to the fifth toe. These findings together with published data showing that α-motor nerve endings begin to degenerate during the asymptomatic phase of the disease (Rocha et al., 2013; Moloney et al., 2014) suggest that peripheral proprioceptive sensory and α-motor axons are similarly affected in SOD1^{G93A} mice. In contrast, we found no structural alterations at NMJs of symptomatic TDP43 mutant mice (Fig. 5C–E) even though proprioceptive sensory nerve endings exhibit structural alterations in these mice. Together, these results indicate that degeneration of peripheral proprioceptive sensory nerve endings occurs independently of defects associated with the somatic motor system.

Ib proprioceptive sensory and γ-motor nerve endings are less affected in SOD1^{G93A} mice

We next sought to determine whether other neurons innervating skeletal muscles are also affected by ALS-causing mutations. In addition to Ia/II proprioceptive sensory and α-motor axons, skeletal muscles are innervated by γ-motor and Ib proprioceptive sensory neurons. Although γ-motor axons innervate AChR clusters located at the polar regions of intrafusal muscles fibers, Ib proprioceptive sensory nerve endings terminate at the interphase between muscle fibers and tendons, where they form Golgi tendons. To determine whether ALS similarly affects these peripheral axons, we examined their architecture in the same muscles from 90-day-old Thy1-YFP and SOD1^{G93A};Thy1-YFP mice used to visualize Ia/II proprioceptive and α-motor nerve endings. We often found γ-motor neurons innervating muscle spindles devoid of Ia/II proprioceptive nerve endings and adjacent to α-motor nerve endings clearly retracting from NMJs in SOD1^{G93A} mice (Fig. 6A,B). Similarly, Ib proprioceptive nerve endings were found innervating Golgi tendons near muscle spindles containing the remnants of degenerated Ia/II nerve endings (Fig. 7A,B). Thus, γ-motor and Ib proprioceptive nerve endings appear to be less affected by expression of SOD1^{G93A} compared with Ia/II proprioceptive sensory and α-motor axons.

Degeneration of proprioceptive synapses in the spinal cord

Based on the findings presented above, we examined Ia/II proprioceptive and cholinergic synapses on α-motor somata in the spinal cord of mutant mice. The majority of inputs containing VGluT1 on α-motor somata are from Ia/II proprioceptive sensory axons (Alvarez et al., 2011), even though VGluT1 also marks synaptic inputs from spinal cord interneurons and descending cortical axons. We therefore used an antibody against VGluT1 to determine the impact of ALS on these synapses. In the same α-motor neuron somata, we examined cholinergic inputs with an antibody against VAChT. For 90-day-old male SOD1^{G93A}, we found a significant loss of VGluT1 and VAChT synapses on the soma of α-motor neurons,

independent of neuronal atrophy, compared with control (Fig. 8A,B,D,E). However, although VGluT1-positive synapses were significantly reduced in 90-day-old TDP43^{A315T} mice (Fig. 8C,E), we found no difference in the number of VAChT-positive synapses compared with control mice (Fig. 8C,D). Together with our observations at the NMJ, these findings further indicate that expression of TDP43^{A315T} has little impact on cholinergic synapses. We then examined 60-day-old SOD1^{G93A} animals to determine whether the loss of VGluT1- and VAChT-positive synapses also precedes the appearance of obvious neurological symptoms in SOD1^{G93A}. Our analysis revealed no difference in the number of VAChT and VGluT1 synapses between 60-day-old SOD1^{G93A} and control mice (Fig. 9A–D). These findings suggest that proprioceptive and cholinergic synapses in the spinal cord are affected after NMJs (Moloney et al., 2014) and muscle sensory afferents innervating spindles degenerate in mice harboring ALS-causing mutations.

DISCUSSION

We examined proprioceptive sensory neurons in two mouse lines carrying ALS-causing mutant genes. We show that Ia/II proprioceptive sensory neurons are affected and provide strong evidence that they are involved in the progression of ALS in two mouse models for the disease, in SOD1^{G93A} and TDP43^{A315T} mice. Ia/II Proprioceptive sensory neurons peripheral nerve terminals exhibit structural abnormalities before the onset of neurological symptoms and degenerate as symptoms arise. These changes occur before the loss of nerve endings in the spinal cord and independently of degeneration of α-motor neuron axons. We reached these conclusions based on 1) analysis of peripheral and central synapses in the same animals and 2) different effects of TDP43 mutant on sensory and cholinergic nerve endings.

During the course of our study, we also discovered that proprioceptive sensory neurons differ in their response to ALS-related insults, with nerve endings from Ia/II proprioceptors degenerating much earlier than those from Ib proprioceptive sensory neurons. We found a similar pattern for α- and γ-motor nerve endings. γ-Axons were often found innervating AChR clusters at the polar region of intrafusal muscle fibers next to partially or completely denervated NMJs. These findings are important for two reasons: First, they indicate that neurons associated with neuromuscular function exhibit different susceptibility to ALS; second, they provide further evidence that cells directly contacting α-motor neurons are preferentially affected in ALS. These findings add to the list of subpopulations of neurons that are uniquely affected by ALS (Saxena et al., 2009; Valdez et al., 2012).

Potential roles of peripheral nerve endings in ALS

ALS is characterized by pathological changes at sites of contact between cells, including at synapses. In muscles, α-motor axon terminals at NMJs have been shown to undergo bouts of degeneration and regeneration in young asymptomatic mice expressing mutant SOD1 (Schaefer et al., 2005). Later in life, motor axons degenerate via a process termed “dying back”, resulting in the appearance of neurological symptoms from denervation of muscle fibers and loss of motor neurons (Dadon-Nachum et al., 2011). In a futile attempt to stave off the disease, skeletal muscles secrete a variety of molecules that function to stabilize the

NMJ and promote nerve regeneration. Among these muscle-secreted molecules are GDNF, VEGF, IGF-1, and semaphorin 3A, and they have been shown to slow degeneration of α-motor axons in ALS-afflicted mice (Sun et al., 2002; De Winter et al., 2006; Dadon-Nachum et al., 2014; Venkova et al., 2014).

As with motor axons, lack of muscle-derived signals results in degeneration of proprioceptive sensory nerve endings (Ernfors et al., 1994; Kucera et al., 1995; Chalazonitis, 1996; Oakley et al., 1997). Proprioceptive sensory neurons require the neurotrophic factor, neurotrophin-3 (NT3), secreted by intrafusal muscle fibers, to develop and maintain their peripheral and central connections and to survive (Ernfors et al., 1994; Kucera et al., 1995; Chalazonitis, 1996). The main receptor for NT3 is the neurotrophic receptor TrkC, which is expressed in proprioceptive sensory neurons (Matsuo et al., 2000). Several other molecules have been shown to be important for the maintenance and regeneration of sensory axons and their nerve endings, including GDNF and VEGF (Krakora et al., 2013; Dadon-Nachum et al., 2014). For muscle-derived secreted factors to help neurons resist ALS-related changes, they must be retrogradely transported together with cognate receptors to the cell body in order to activate prosurvival and maintenance signals. Although retrograde transport was found to be normal in the sensory branch of saphenous nerve in $SOD1^{G93A}$ mice (Marinkovic et al., 2012), this branch is devoid of Ia/II proprioceptive sensory axons. Thus, future studies should assess the levels of muscle-derived factors and whether they are in fact retrogradely transported up the axon of Ia/II proprioceptive sensory neurons expressing mutant genes known to cause ALS.

Potential roles of central nerve endings in ALS

In the central nervous system, connections between cells are disrupted and are believed to contribute to the initiation and progression of ALS, including synapses that α-motor neurons form with descending cortical motor axons, Renshaw and small cholinergic neurons (Ozdinler et al., 2011; Wootz et al., 2013; Gallart-Palau et al., 2014). Here we validate published results indicating that motor neurons are stripped of VAChT and VGluT1 synapses in symptomatic $SOD1^{G93A}$ mice (Schütz, 2005; Gallart-Palau et al., 2014). We also show that Ia/II proprioceptive sensory synapses with α-motor neurons are also affected in $SOD1^{G93A}$ and $TDP43^{A315T}$ mice. Although our data indicate that degeneration of peripheral proprioceptive nerve endings precedes loss of connections with motor neurons, we cannot exclude the possibility that spinal cord synapses undergo bouts of degeneration and regeneration during the presymptomatic phase of the disease, as observed in muscles. In fact, it has been shown via electron microscopy that motor neuron presynapses on Renshaw cells are altered in presymptomatic $SOD1^{G93A}$ mice (Wootz et al., 2013). Moreover, our analysis relied on confocal images, which lack the resolution needed to reveal subcellular synaptic structural changes in spinal cord synapses because they are significantly smaller compared with Ia/II afferents at muscle spindles and NMJs. Nevertheless, our results show that peripheral and central proprioceptive nerve endings are affected in ALS-afflicted mice, further suggesting that pathological changes at sites of contact between cells may disrupt cellular homeostasis, leading to degeneration of axons followed by neuronal death.

Similarities and differences between proprioceptive sensory and motor neurons

Ia/II Proprioceptive sensory and α-motor axons share many features: they are the largest neurons in their surroundings; they send long axons to contact muscle fibers in the periphery; they depend on trophic support from muscle fibers to develop and survive; and they form monosynaptic connections in the spinal cord. Interestingly, two recent publications have shown that Ia/II proprioceptive sensory neurons express and localize key molecules needed to form and maintain the NMJ, revealing additional features shared by these two types of neurons (ZhaNg et al., 2014, 2015). In stark contrast to the soma of α-motor neurons, which exhibits numerous pathological changes in presymptomatic $SOD1^{G93A}$ mice (Feeney et al., 2001), our analysis indicates that the soma of proprioceptive sensory neurons, in addition to all other sensory neurons in DRGs, resist degeneration during the early stages of the disease.

There are major differences between proprioceptive sensory and motor neurons. To start, these neurons reside in different anatomical regions, and there is little evidence indicating that Schwann cells and peripheral cells, which directly interact with proprioceptive sensory neurons, are affected by ALS-causing mutations. On the contrary, site-specific removal of mutant SOD1 from Schwann cells worsens disease progression in mice (Lobsiger et al., 2009). Hence, sensory neurons may inhabit an environment that allows them to remain viable for much longer during the progression of ALS. In contrast, motor neurons are surrounded by a wide range of cells known to be affected and play active roles in accelerating the progression of ALS, including glial and other spinal cord neurons (Boillée et al., 2006a). Additionally, α-motor neurons receive inputs from descending cortical neurons also affected and involved in ALS (Ozdinler et al., 2011). Thus, unlike sensory neurons, α-motor neurons have been shown to be affected by dysfunction in partnering cells, suspected of releasing and spreading toxic molecules in a “prion-like” manner at sites of contact, including synapses (Münch et al., 2011).

Our analysis also reveals that Ib proprioceptive sensory and γ-motor neurons nerve endings are spared in muscle fibers. These neuronal subtypes have unique features that may allow them to resist ALS-driven degeneration. Unlike Ia afferents, Ib proprioceptive nerve endings innervate collagen fibrils in skeletal muscles. Thus, they are likely better insulated from toxic factors secreted by atrophying extrafusal and intrafusal muscles fibers. The differences between γ-and α-motor neurons are more obvious. These two cells serve very different functions; the cell bodies of γ-motor neurons are significantly smaller and lack direct input from Ia/II proprioceptive sensory neurons. These anatomical features along with unique molecular machineries may underlie the different susceptibility of Ib sensory and γ-motor neurons to ALS.

Significance to advancing ALS research

Ia/II Proprioceptive sensory neurons play a central role in the monosynaptic stretch reflex, and degeneration of their nerve endings would inevitably result in significant motor deficiencies. However, it is less clear how loss of proprioceptive sensory nerve endings affects the ability of α-motor neurons to withstand ALS-related cellular damages. Given that hyperactivity, in part by unchecked calcium influx via glutamate dependent channels, is

suspected of causing degeneration of α-motor neurons, loss of Ia/II afferents should presumably make motor neurons less excitable and hence help them to resist ALS (Heath and Shaw, 2002). This hypothesis, however, is not supported by our findings. Another possibility is that proprioceptive sensory neuron inputs are required to maintain optimal function and health of α-motor neurons. In this regard, it has been shown that loss of muscle spindles, and hence NT3 support for innervating afferents, results in functional deficits between sensory and motor connections (Chen et al., 2002). Similarly, loss of motor neuron-derived NT3 results in degeneration of sensory inputs in the spinal cord along with apoptosis of the neurons in DRGs (Chen et al., 2002; Usui et al., 2012).

To define better the role of proprioceptive sensory neurons and their role in the survival of α-motor neurons in ALS, transgenic mice expressing or lacking $SOD1^{G93A}$ selectively in proprioceptive sensory neurons will have to be analyzed. Unlike motor neurons, these sensory neurons can be isolated from animals at any stage of their lives and kept in culture for weeks. This feature should make it possible to determine the impact of ALS-causing mutant genes specifically on the molecular composition, biophysical properties, and survival of cultured proprioceptive sensory neurons. Hence, these cells could prove to be a useful model system for identifying and testing therapeutics that can slow or stop axonal degeneration caused by expression of ALS-causing mutant genes.

Acknowledgments

Grant sponsor: This work was supported by a National Institute of Health/NINDS (5K01NS085071-03; GV), by a Virginia Tech Undergraduate Research Fellowship (SURF; SKV and ZK) and an ACC Academic Consortium for Creativity and Innovations fellowship (SKV).

The authors thank members of the Valdez laboratory, in particular Milagros Tenga, for intellectual input on experiments and comments on the manuscript.

ROLE OF AUTHORS

All authors had full access to all the data in the study and take responsibility for the integrity of the data and the accuracy of the data analysis. Study concept and design: SKV, GV. Acquisition of data: SKV, ZK, TH, FV, GV. Analysis and interpretation of data: SKV, ZK, GV. Drafting of the manuscript: SKV, GV. Critical revision of the manuscript for important intellectual content: SKV, TH, FV, GV. Statistical analysis: SKV, GV. Obtained funding: SKV, ZK. Administrative, technical, and material support: SKV, ZK, TH, FV, GV. Study supervision: GV.

LITERATURE CITED

Alvarez FJ, Titus-Mitchell HE, Bullinger KL, Kraszpulski M, Nardelli P, Cope TC. Permanent central synaptic disconnection of proprioceptors after nerve injury and regeneration. I. Loss of VGLUT1/IA synapses on motoneurons. J Neurophysiol. 2011; 106:2450–2470. [PubMed: 21832035]

Balaram P, Isaamullah M, Petry HM, Bickford ME, Kaas JH. Distributions of vesicular glutamate transporters 1 and 2 in the visual system of tree shrews (*Tupaia belangeri*). J Comp Neurol. 2015; 523:1792–1808. [PubMed: 25521420]

Boillée S, Vande Velde C, Cleveland DW. ALS: a disease of motor neurons and their nonneuronal neighbors. Neuron. 2006a; 52:39–59. [PubMed: 17015226]

Boillée S, Yamanaka K, Lobsiger CS, Copeland NG, Jenkins NA, Kassiotis G, Kollias G, Cleveland DW. Onset and progression in inherited ALS determined by motor neurons and microglia. Science. 2006b; 312:1389–1392. [PubMed: 16741123]

Bradley WG, Good P, Rasool CG, Adelman LS. Morphometric and biochemical studies of peripheral nerves in amyotrophic lateral sclerosis. Ann Neurol. 1983; 14:267–277. [PubMed: 6195954]

Buffelli M, Burgess RW, Feng G, Lobe CG, Lichtman JW, Sanes JR. Genetic evidence that relative synaptic efficacy biases the outcome of synaptic competition. Nature. 2003; 424:430–434. [PubMed: 12879071]

Chalazonitis A. Neurotrophin-3 as an essential signal for the developing nervous system. Mol Neurobiol. 1996; 12:39–53. [PubMed: 8732539]

Chen H-H, Tourtellotte WG, Frank E. Muscle spindle-derived neurotrophin 3 regulates synaptic connectivity between muscle sensory and motor neurons. J Neurosci. 2002; 22:3512–3519. [PubMed: 11978828]

Cooper AP, Gillespie DC. Synaptotagmins I and II in the developing rat auditory brainstem: Synaptotagmin I is transiently expressed in glutamate-releasing immature inhibitory terminals. J Comp Neurol. 2011; 519:2417–2433. [PubMed: 21456023]

Dadon-Nachum M, Melamed E, Offen D. The “dying-back” phenomenon of motor neurons in ALS. J Mol Neurosci. 2011; 43:470–477. [PubMed: 21057983]

Dadon-Nachum M, Ben-Yaacov K, Ben-Zur T, Barhum Y, Yaffe D, Perlson E, Offen D. Transplanted modified muscle progenitor cells expressing a mixture of neurotrophic factors delay disease onset and enhance survival in the SOD1 mouse model of ALS. J Mol Neurosci. 2014; 55:788–797. [PubMed: 25330859]

De Winter F, Vo T, Stam FJ, Wisman LAB, Bär PR, Niclou SP, van Muiswinkel FL, Verhaagen J. The expression of the chemorepellent semaphorin 3A is selectively induced in terminal Schwann cells of a subset of neuromuscular synapses that display limited anatomical plasticity and enhanced vulnerability in motor neuron disease. Mol Cell Neurosci. 2006; 32:102–117. [PubMed: 16677822]

Duplan L, Bernard N, Casseron W, Dudley K, Thouvenot E, Honnorat J, Rogemond V, De Bovis B, Aebischer P, Marin P, Raoul C, Henderson CE, Pettmann B. Collapsin response mediator protein 4a (CRMP4a) is upregulated in motoneurons of mutant SOD1 mice and can trigger motoneuron axonal degeneration and cell death. J Neurosci. 2010; 30:785–796. [PubMed: 20071543]

Dyck PJ, Stevens JC, Mulder DW, Espinosa RE. Frequency of nerve fiber degeneration of peripheral motor and sensory neurons in amyotrophic lateral sclerosis. Morphometry of deep and superficial peroneal nerves. Neurology. 1975; 25:781–785. [PubMed: 1171412]

Enjin A, Rabe N, Nakanishi ST, Vallstedt A, Gezelius H, Memic F, Lind M, Hjalt T, Tourtellotte WG, Bruder C, Eichele G, Whelan PJ, Kullander K. Identification of novel spinal cholinergic genetic subtypes disclose Chodl and Pitx2 as markers for fast motor neurons and partition cells. J Comp Neurol. 2010; 518:2284–2304. [PubMed: 20437528]

Ernfors P, Lee KF, Kucera J, Jaenisch R. Lack of neurotrophin-3 leads to deficiencies in the peripheral nervous system and loss of limb proprioceptive afferents. Cell. 1994; 77:503–512. [PubMed: 7514502]

Feeney SJ, McKelvie PA, Austin L, Jean-Francois MJ, Kapsa R, Tombs SM, Byrne E. Presymptomatic motor neuron loss and reactive astrocytosis in the SOD1 mouse model of amyotrophic lateral sclerosis. Muscle Nerve. 2001; 24:1510–1519. [PubMed: 11745954]

Feng G, Mellor RH, Bernstein M, Keller-Peck C, Nguyen QT, Wallace M, Nerbonne JM, Lichtman JW, Sanes JR. Imaging neuronal subsets in transgenic mice expressing multiple spectral variants of GFP. Neuron. 2000; 28:41–51. [PubMed: 11086982]

Fox MA, Sanes JR. Synaptotagmin I and II are present in distinct subsets of central synapses. J Comp Neurol. 2007; 503:280–296. [PubMed: 17492637]

Gallart-Palau X, Tarabal O, Casanovas A, Sábado J, Correa FJ, Hereu M, Piedrafita L, Calderó J, Esquerda JE. Neuregulin-1 is concentrated in the postsynaptic subsurface cistern of C-bouton inputs to α-motoneurons and altered during motoneuron diseases. FASEB J. 2014; 28:3618–3632. [PubMed: 24803543]

Garbelli R, Inverardi F, Medici V, Amadeo A, Verderio C, Matteoli M, Frassoni C. Heterogeneous expression of SNAP-25 in rat and human brain. J Comp Neurol. 2008; 506:373–386. [PubMed: 18041776]

Guo YS, Wu DX, Wu HR, Wu SY, Yang C, Li B, Bu H, Zhang YS, Li CY. Sensory involvement in the SOD1-G93A mouse model of amyotrophic lateral sclerosis. Exp Mol Med. 2009; 41:140–150. [PubMed: 19293633]

Gurney ME, Pu H, Chiu AY, Dal Canto MC, Polchow CY, Alexander DD, Caliendo J, Hentati A, Kwon YW, Deng HX. Motor neuron degeneration in mice that express a human Cu,Zn superoxide dismutase mutation. Science. 1994; 264:1772–1775. [PubMed: 8209258]

Haidet-Phillips AM, Hester ME, Miranda CJ, Meyer K, Braun L, Frakes A, Song S, Likhite S, Murtha MJ, Foust KD, Rao M, Eagle A, Kammesheidt A, Christensen A, Mendell JR, Burghes AHM, Kaspar BK. Astrocytes from familial and sporadic ALS patients are toxic to motor neurons. Nat Biotechnol. 2011; 29:824–828. [PubMed: 21832997]

Hammad M, Silva A, Glass J, Sladky JT, Benatar M. Clinical, electrophysiologic, and pathologic evidence for sensory abnormalities in ALS. Neurology. 2007; 69:2236–2242. [PubMed: 18071143]

Hanyu N, Oguchi K, Yanagisawa N, Tsukagoshi H. Degeneration and regeneration of ventral root motor fibers in amyotrophic lateral sclerosis. Morphometric studies of cervical ventral roots. J Neurol Sci. 1982; 55:99–115. [PubMed: 7108564]

Hardiman O, van den Berg LH, Kiernan MC. Clinical diagnosis and management of amyotrophic lateral sclerosis. Nat Rev Neurol. 2011; 7:639–649. [PubMed: 21989247]

Harrington AM, Brierley SM, Isaacs N, Hughes PA, Castro J, Blackshaw LA. Sprouting of colonic afferent central terminals and increased spinal mitogen-activated protein kinase expression in a mouse model of chronic visceral hypersensitivity. J Comp Neurol. 2012; 520:2241–2255. [PubMed: 22237807]

Hatzipetros T, Bogdanik LP, Tassinari VR, Kidd JD, Moreno AJ, Davis C, Osborne M, Austin A, Vieira FG, Lutz C, Perrin S. C57BL/6J congenic Prp-TDP43A315T mice develop progressive neurodegeneration in the myenteric plexus of the colon without exhibiting key features of ALS. Brain Res. 2014; 1584:59–72. [PubMed: 24141148]

Heath PR, Shaw PJ. Update on the glutamatergic neurotransmitter system and the role of excitotoxicity in amyotrophic lateral sclerosis. Muscle Nerve. 2002; 26:438–458. [PubMed: 12362409]

Hippenmeyer S, Vrieseling E, Sigrist M, Portmann T, Laengle C, Ladle DR, Arber S. A developmental switch in the response of DRG neurons to ETS transcription factor signaling. PLoS Biol. 2005; 3:e159. [PubMed: 15836427]

Jaarsma D, Teuling E, Haasdijk ED, De Zeeuw CI, Hoogenraad CC. Neuron-specific expression of mutant superoxide dismutase is sufficient to induce amyotrophic lateral sclerosis in transgenic mice. J Neurosci. 2008; 28:2075–2088. [PubMed: 18305242]

Krakora D, Mulcrone P, Meyer M, Lewis C, Bernau K, Gowing G, Zimprich C, Aebischer P, Svendsen CN, Suzuki M. Synergistic effects of GDNF and VEGF on lifespan and disease progression in a familial ALS rat model. Mol Ther. 2013; 21:1602–1610. [PubMed: 23712039]

Kucera J, Fan G, Jaenisch R, Linnarsson S, Ernfors P. Dependence of developing group Ia afferents on neuro-trophin-3. J Comp Neurol. 1995; 363:307–320. [PubMed: 8642077]

Lai K-O, Zhao Y, Ch'ng TH, Martin KC. Importin-mediated retrograde transport of CREB2 from distal processes to the nucleus in neurons. Proc Natl Acad Sci U S A. 2008; 105:17175–17180. [PubMed: 18957537]

Lawson SN. The postnatal development of large light and small dark neurons in mouse dorsal root ganglia: a statistical analysis of cell numbers and size. J Neurocytol. 1979; 8:275–294. [PubMed: 490184]

Ling S-C, Polymenidou M, Cleveland DW. Converging mechanisms in ALS and FTD: disrupted RNA and protein homeostasis. Neuron. 2013; 79:416–438. [PubMed: 23931993]

Lobsiger CS, Boillee S, McAlonis-Downes M, Khan AM, Feltri ML, Yamanaka K, Cleveland DW. Schwann cells expressing dismutase active mutant SOD1 unexpectedly slow disease progression in ALS mice. Proc Natl Acad Sci U S A. 2009; 106:4465–4470. [PubMed: 19251638]

Marinkovic P, Reuter MS, Brill MS, Godinho L, Kerschensteiner M, Misgeld T. Axonal transport deficits and degeneration can evolve independently in mouse models of amyotrophic lateral sclerosis. Proc Natl Acad Sci U S A. 2012; 109:4296–4301. [PubMed: 22371592]

Matsuo S, Ichikawa H, Silos-Santiago I, Arends JJ, Henderson TA, Kiyomiya K, Kurebe M, Jacquin MF. Proprioceptive afferents survive in the masseter muscle of trkC knockout mice. Neuroscience. 2000; 95:209–216. [PubMed: 10619477]

McMahon SB, Armanini MP, Ling LH, Phillips HS. Expression and coexpression of Trk receptors in subpopulations of adult primary sensory neurons projecting to identified peripheral targets. Neuron. 1994; 12:1161–1171. [PubMed: 7514427]

Mead RJ, Bennett EJ, Kennerley AJ, Sharp P, Sunyach C, Kasher P, Berwick J, Pettmann B, Battaglia G, Azzouz M, Grierson A, Shaw PJ. Optimised and rapid pre-clinical screening in the SOD1(G93A) transgenic mouse model of amyotrophic lateral sclerosis (ALS). PLoS One. 2011; 6:e23244. [PubMed: 21876739]

Mentis GZ, Blivis D, Liu W, Drobac E, Crowder ME, Kong L, Alvarez FJ, Sumner CJ, O'Donovan MJ. Early functional impairment of sensory-motor connectivity in a mouse model of spinal muscular atrophy. Neuron. 2011; 69:453–467. [PubMed: 21315257]

Mochizuki Y, Mizutani T, Shimizu T, Kawata A. Proportional neuronal loss between the primary motor and sensory cortex in amyotrophic lateral sclerosis. Neurosci Lett. 2011; 503:73–75. [PubMed: 21871950]

Moloney EB, de Winter F, Verhaagen J. ALS as a distal axonopathy: molecular mechanisms affecting neuromuscular junction stability in the presymptomatic stages of the disease. Front Neurosci. 2014; 8:252. [PubMed: 25177267]

Mullen RJ, Buck CR, Smith AM. NeuN, a neuronal specific nuclear protein in vertebrates. Development. 1992; 116:201–211. [PubMed: 1483388]

Münch C, O'Brien J, Bertolotti A. Prion-like propagation of mutant superoxide dismutase-1 misfolding in neuronal cells. Proc Natl Acad Sci U S A. 2011; 108:3548–3553. [PubMed: 21321227]

Neumann M, Sampathu DM, Kwong LK, Truax AC, Micsenyi MC, Chou TT, Bruce J, Schuck T, Grossman M, Clark CM, McCluskey LF, Miller BL, Masliah E, Mackenzie IR, Feldman H, Feiden W, Kretzschmar HA, Trojanowski JQ, Lee VM-Y. Ubiquitinated TDP-43 in frontotemporal lobar degeneration and amyotrophic lateral sclerosis. Science. 2006; 314:130–133. [PubMed: 17023659]

Ng ASL, Rademakers R, Miller BL. Frontotemporal dementia: a bridge between dementia and neuromuscular disease. Ann N Y Acad Sci. 2015; 1338:71–93. [PubMed: 25557955]

Oakley RA, Lefcort FB, Clary DO, Reichardt LF, Prevette D, Oppenheim RW, Frank E. Neurotrophin-3 promotes the differentiation of muscle spindle afferents in the absence of peripheral targets. J Neurosci. 1997; 17:4262–4274. [PubMed: 9151743]

Ozdinler PH, Benn S, Yamamoto TH, Güzel M, Brown RH, Macklis JD. Corticospinal motor neurons and related subcerebral projection neurons undergo early and specific neurodegeneration in hSOD1G^{93}A transgenic ALS mice. J Neurosci. 2011; 31:4166–4177. [PubMed: 21411657]

Petralia RS, Schwartz CM, Wang Y-X, Mattson MP, Yao PJ. Subcellular localization of Patched and Smoothened, the receptors for Sonic hedgehog signaling, in the hippocampal neuron. J Comp Neurol. 2011; 519:3684–3699. [PubMed: 21618238]

Philips T, Rothstein JD. Glial cells in amyotrophic lateral sclerosis. Exp Neurol. 2014; 262PB:111–120.

Pradat P-F, El Mendili M-M. Neuroimaging to investigate multisystem involvement and provide biomarkers in amyotrophic lateral sclerosis. Biomed Res Int. 2014; 2014:467560. [PubMed: 24949452]

Pugdahl K, Fuglsang-Frederiksen A, de Carvalho M, Johnsen B, Fawcett PRW, Labarre-Vila A, Liguori R, Nix WA, Schofield IS. Generalised sensory system abnormalities in amyotrophic lateral sclerosis: a European multicentre study. J Neurol Neurosurg Psychiatry. 2007; 78:746–749. [PubMed: 17575020]

Rocha MC, Pousinha PA, Correia AM, Sebastião AM, Ribeiro JA. Early changes of neuromuscular transmission in the SOD1(G93A) mice model of ALS start long before motor symptoms onset. PLoS One. 2013; 8:e73846. [PubMed: 24040091]

Sábado J, Casanovas A, Tarabal O, Hereu M, Piedrafita L, Calderó J, Esquerda JE. Accumulation of misfolded SOD1 in dorsal root ganglion degenerating proprioceptive sensory neurons of transgenic mice with amyotrophic lateral sclerosis. Biomed Res Int. 2014; 2014:852163. [PubMed: 24877142]

Saxena S, Cabuy E, Caroni P. A role for motoneuron subtype-selective ER stress in disease manifestations of FALS mice. Nat Neurosci. 2009; 12:627–636. [PubMed: 19330001]

Schaefer AM, Sanes JR, Lichtman JW. A compensatory sub-population of motor neurons in a mouse model of amyotrophic lateral sclerosis. J Comp Neurol. 2005; 490:209–219. [PubMed: 16082680]

Schütz B. Imbalanced excitatory to inhibitory synaptic input precedes motor neuron degeneration in an animal model of amyotrophic lateral sclerosis. Neurobiol Dis. 2005; 20:131–140. [PubMed: 16137574]

Scott BB, Lois C. Developmental origin and identity of song system neurons born during vocal learning in songbirds. J Comp Neurol. 2007; 502:202–214. [PubMed: 17348018]

Sternberger LA, Harwell LW, Sternberger NH. Neurotypy: regional individuality in rat brain detected by immunocytochemistry with monoclonal antibodies. Proc Natl Acad Sci U S A. 1982; 79:1326–1330. [PubMed: 7041117]

Sun W, Funakoshi H, Nakamura T. Overexpression of HGF retards disease progression and prolongs life span in a transgenic mouse model of ALS. J Neurosci. 2002; 22:6537–6548. [PubMed: 12151533]

Trevarrow B, Marks DL, Kimmel CB. Organization of hindbrain segments in the zebrafish embryo. Neuron. 1990; 4:669–679. [PubMed: 2344406]

Usui N, Watanabe K, Ono K, Tomita K, Tamamaki N, Ikenaka K, Takebayashi H. Role of motoneuron-derived neurotrophin 3 in survival and axonal projection of sensory neurons during neural circuit formation. Development. 2012; 139:1125–1132. [PubMed: 22318233]

Valdez G, Tapia JC, Lichtman JW, Fox MA, Sanes JR. Shared resistance to aging and ALS in neuromuscular junctions of specific muscles. PLoS One. 2012; 7:e34640. [PubMed: 22485182]

Venkova K, Christov A, Kamaluddin Z, Kobalka P, Siddiqui S, Hensley K. Semaphorin 3A signaling through neuropilin-1 is an early trigger for distal axonopathy in the SOD1G93A mouse model of amyotrophic lateral sclerosis. J Neuropathol Exp Neurol. 2014; 73:702–713. [PubMed: 24918638]

Wegorzewska I, Bell S, Cairns NJ, Miller TM, Baloh RH. TDP-43 mutant transgenic mice develop features of ALS and frontotemporal lobar degeneration. Proc Natl Acad Sci U S A. 2009; 106:18809–18814. [PubMed: 19833869]

Wootz H, Fitzsimons-Kantamneni E, Larhammar M, Rotterman TM, Enjin A, Patra K, André E, Van Zundert B, Kullander K, Alvarez FJ. Alterations in the motor neuron-renshaw cell circuit in the Sod1(G93A) mouse model. J Comp Neurol. 2013; 521:1449–1469.

Zhang Y, Wesolowski M, Karakatsani A, Witzemann V, Kröger S. Formation of cholinergic synapse-like specializations at developing murine muscle spindles. Dev Biol. 2014; 393:227–235. [PubMed: 25064185]

Zhang Y, Lin S, Karakatsani A, Rüegg MA, Kröger S. Differential regulation of AChR clustering in the polar and equatorial region of murine muscle spindles. Eur J Neurosci. 2015; 41:69–78. [PubMed: 25377642]

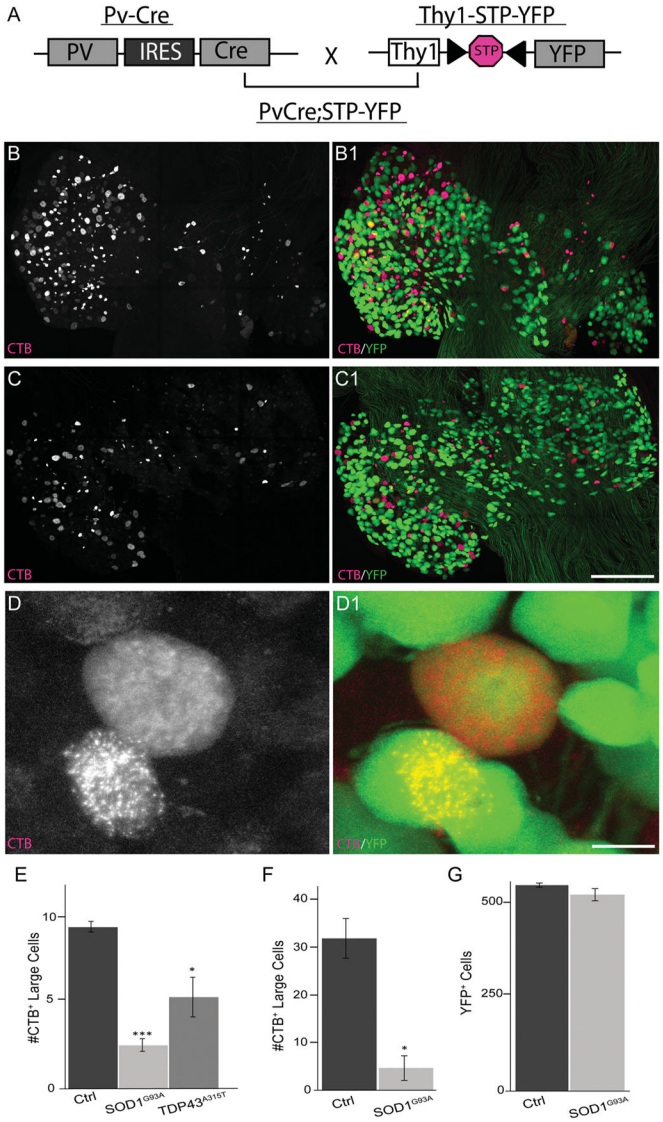

Figure 1.

Fewer proprioceptive sensory neurons innervate the tibialis anterior muscle in SOD1^{G93A} and TDP43^{A315T}. We generated mice expressing YFP selectively in proprioceptive sensory neurons within DRGs (**A–B,D**) and then crossed this new mouse line with SOD1^{G93A} transgenic mice (**C**). Proprioceptive sensory neurons were identified in TDP43^{A315T} mice with NeuN and based on their large soma (see Fig. 2). Five days after focally injecting fCTB into the TA muscle, fewer sensory neurons were found in L3 DRGs of SOD1^{G93A} (n = 8) and TDP43^{A315T} (n = 4) compared with control (n = 5) mice (**B–E**) at 90 days of age. Fewer proprioceptive sensory neurons were also found in SOD1^{G93A} mice injected with fCTB into multiple locations of the TA (**F**). Despite these differences, the same numbers of YFP-positive neurons were found in L3 DRGs from SOD1^{G93A} mice as in control mice (**G**). Only male mice were used for this analysis. Error bar = standard error (STE). *$P < 0.05$ (**E–F**), ***$P < 0.001$ (**E**). Scale bars = 50 μm in C1 (applies to B–C1), 25 μm in D1 (applies to D,D1).

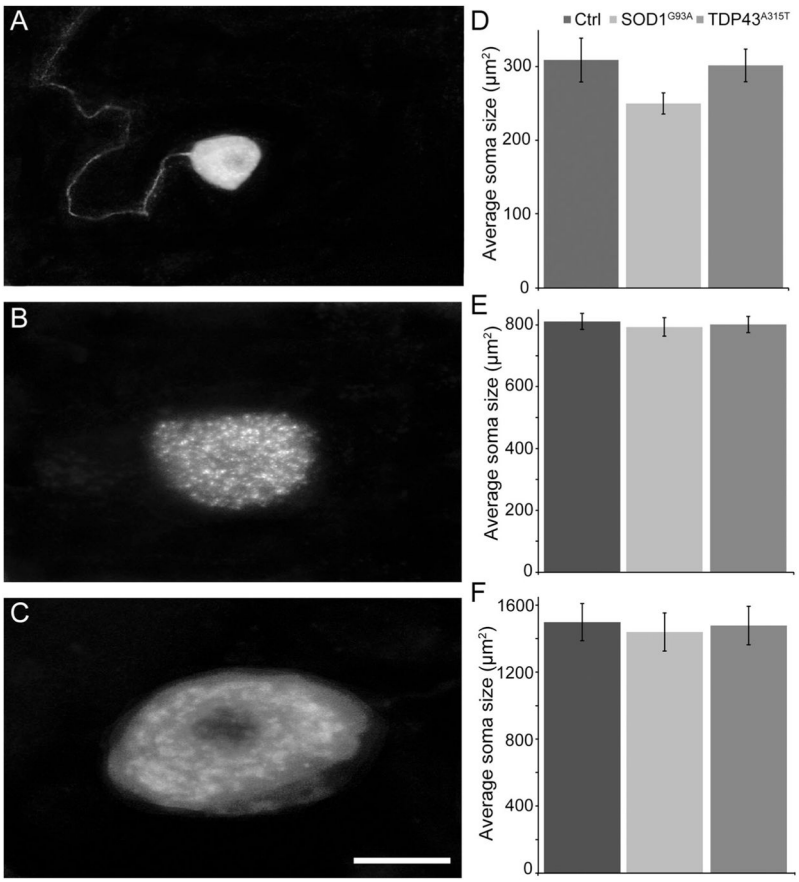

Figure 2.

Sensory somata appear normal in SOD1^{G93A} and TDP43^{A315T} mice. Sensory somata labeled with fCTB were separated into three categories according to size (**A–C**). There is no difference in the average soma size for small (**A,D**), medium-sized (**B,E**), or large (**C,F**) sensory neurons among controls (n = 5), SOD1^{G93A} (n = 8), and TDP43^{A315T} (n = 4) mice at 90 days of age. Only male mice were used for this analysis. Error bar = standard error (STE). Scale bar = 25 μm.

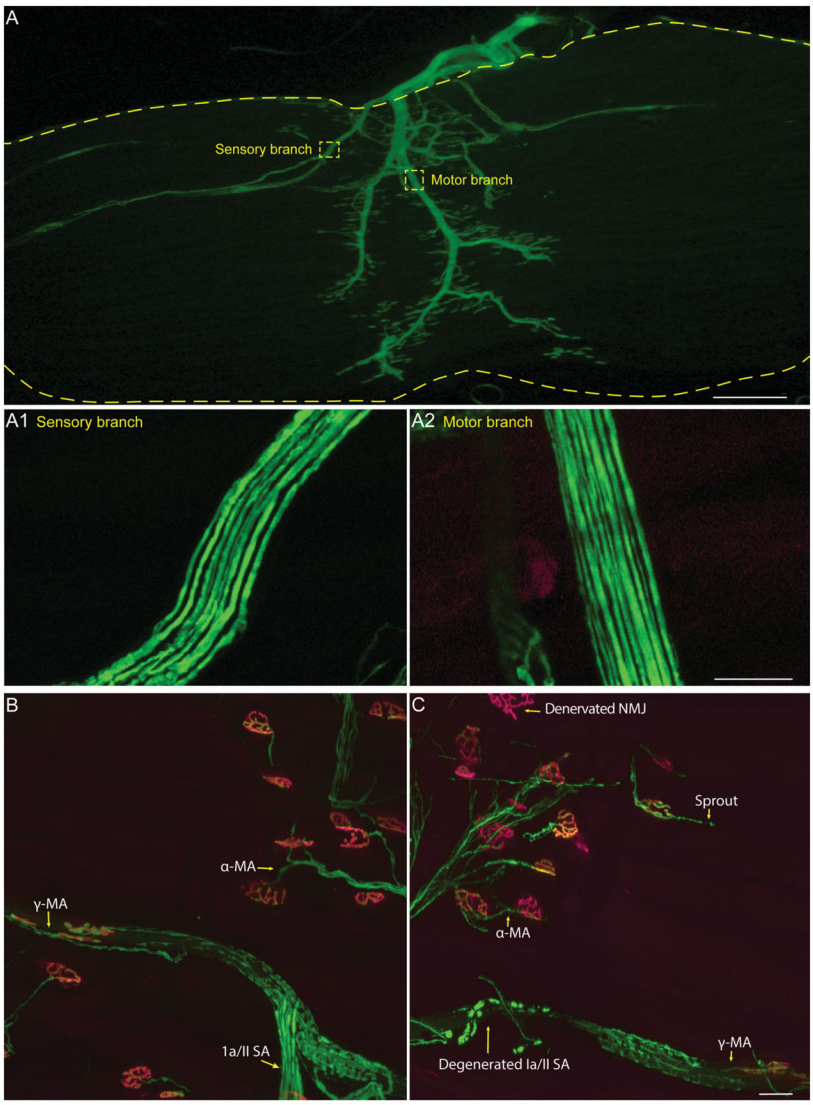

Figure 3.

Visualizing sensory and motor axons in the EDL muscle. Most nerve endings can be fully visualized in whole-mounted EDL muscles from mice expressing YFP (**A**). Sensory (**A1**) and motor (**A2**) branches can be traced from their nerve endings and counted. The nerve endings are shown in control (**B**) and $SOD1^{G93A}$ (**C**) animals. α-MA = α-motor neuron axon; γ-MA = γ-motor neuron axon; Ia/II SA = Ia/II sensory afferent; NMJ, neuromuscular junction.

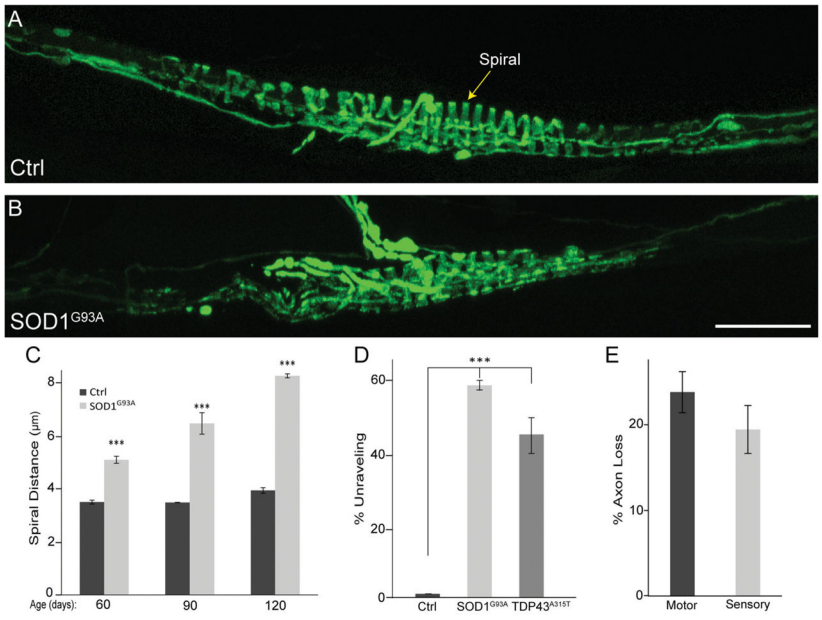

Figure 4.

Peripheral proprioceptive nerve endings degenerate in SOD1^{G93A} and TDP43^{A315T} mice. In control, Ia proprioceptive sensory annulospiral endings are characterized by regular spacing of their spirals (**A**; arrow in **C**), and at least 10 spirals are found wrapping around the equatorial region of the muscle (**A,D**). In SOD1^{G93A}, the distance between spirals increases (**B–C**), and fewer spirals are found around the equatorial region of the muscle (**B,D**). Fewer spirals were also found in TDP43 mutants at 90 days of age (**D**). Proprioceptive sensory axons begin to degenerate alongside α-motor neuron axons during the early phase of the disease (**E**). At least six mice were used at each age. All animals were male; control n = 12, SOD1^{G93A} n = 16, TDP43^{A315T} n = 6. Error bar = STE. ***$P < 0.001$. Scale bar = 50 μm.

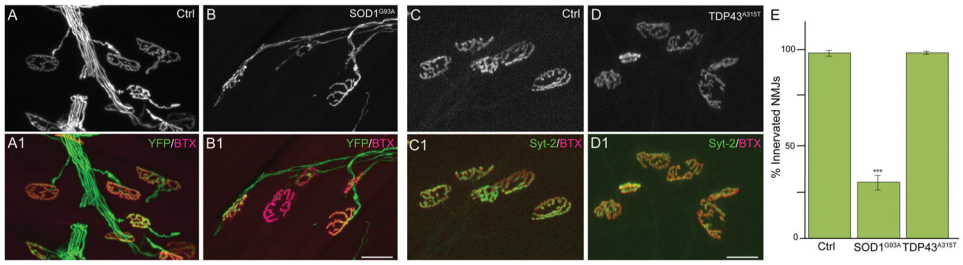

Figure 5.

NMJs are affected in early symptomatic SOD1^{G93A} but not TDP43^{A315T} mice. NMJs were examined in 90-day-old male control (**A1**) and SOD1^{G93A} (**B1**) mice expressing YFP (**A–B**). AChR clusters (red) were labeled with fBTX (**A1–B1**). NMJs of male control (**C1**) and TDP43^{A315T} (**D1**) mice were also examined at 90 days of age by labeling the presynapse with synaptotagmin (**C–D**). NMJs are spared in TDP43^{A315T} (**C–D1,E**) but affected in SOD1^{G93A} mice (**A–B1,E**). At least 50 NMJs were counted per mouse, and five animals were examined per group. Error bar = STE. ***$P < 0.001$. Scale bars = 20 μm in B1 (applies to A–B1), 20 μm in D1 (applies to C–D1).

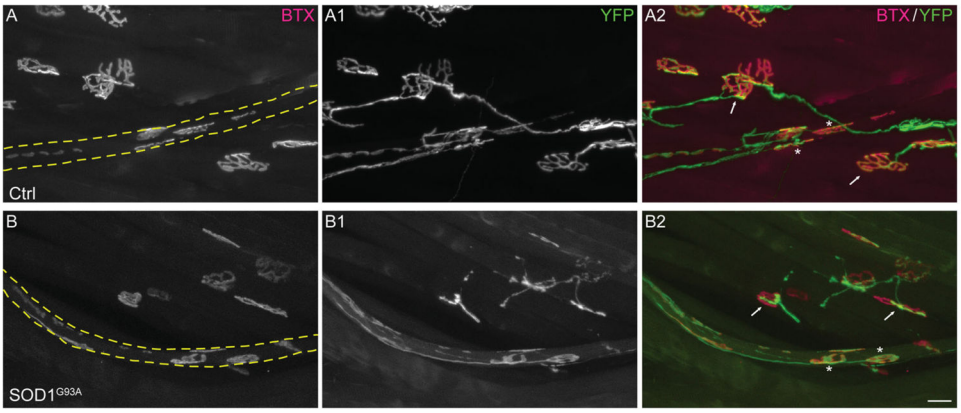

Figure 6.

Analysis of γ-motor axons in SOD1^{G93A} mice. Representative images of γ-motor axons (green) innervating AChR clusters (red) located at the polar region of intrafusal muscle fibers (outlined by the dashed lines) in 90-day-old control (**A–A2**) and SOD1^{G93A} (**B–B2**) mice. The apposition of γ-motor axon with AChR clusters (stars) is unchanged in SOD1^{G93A} compared with control mice (**A2,B2**) even though α-motor axons are clearly retracting from NMJs (arrows). Scale bar = 20 μm.

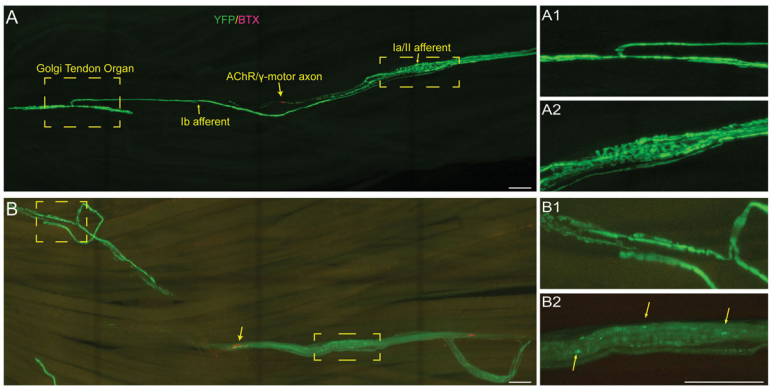

Figure 7.

Analysis of Ib proprioceptive axons in SOD1^{G93A} mice. Representative images of Ib proprioceptive axons (Ib afferent; **A–A1**,**B–B1**) alongside Ia/II proprioceptive sensory axons (Ia/II afferent; **A–A2,B–B2**) in the EDL muscle of 110-day-old control (**A**) and SOD1^{G93A} (**B**) mice. Ib nerve endings are readily found innervating Golgi tendons (**B–B1**) in muscles where Ia/II nerve endings have mostly degenerated (**B,B2**). Scale bars = 50 μm in A,B; 50 μm in B2 (applies to A1–B2).

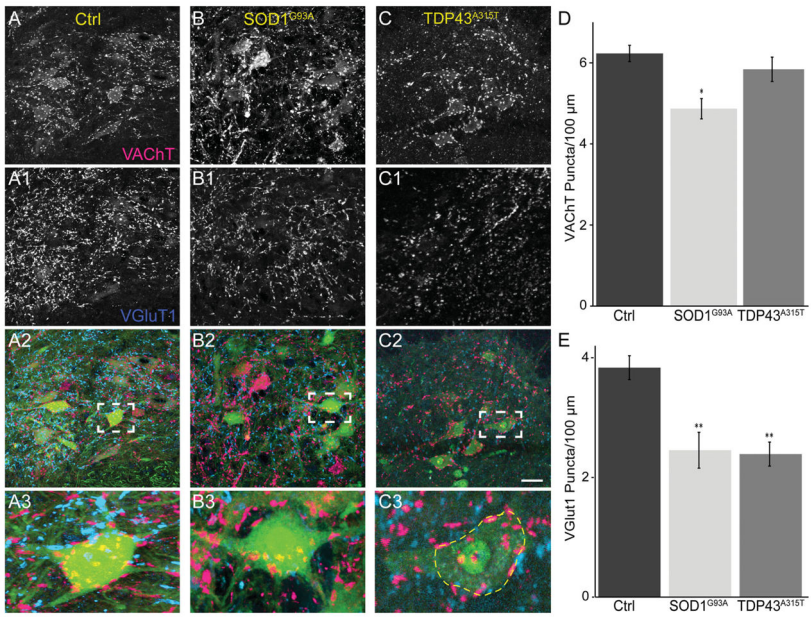

Figure 8.

Loss of VGluT1-positive synapses in the spinal cord of symptomatic SOD1^{G93A} and TDP43^{A315T} mice. Spinal cords at lumbar region 1 from male 90-day-old control (**A**), SOD1^{G93A} (**B**), and TDP43^{A315T} (**C**) mice were stained with VAChT (red) to label cholinergic synapses and VGluT1 (blue) to label proprioceptive synapses. The soma of α-motor neurons were marked by YFP in control and SOD1^{G93A} mice (**A2–A3, B2–B3**; green). The soma of neurons in TDP43^{A315T} mice were labeled with NeuN (**C2–C3**; green). When normalized to the perimeter of the motor neuron soma, there is a significant decrease in cholinergic synapses in SOD1^{G93A} mice (**B,D**) but not TDP43^{A315T} (**C–D**) compared with control mice (**A,D**). VGluT1-positive synapses, however, were reduced in both SOD1^{G93A} (**B1,E**) and TDP43^{A315T} (**C1,D**), mice. At least three animals were examined per group. Error bar = STE. *$P < 0.05$, **$P < 0.01$. Scale bar = 100 µm in C2 (applies to A–C2); 20 µm for A3–C3.

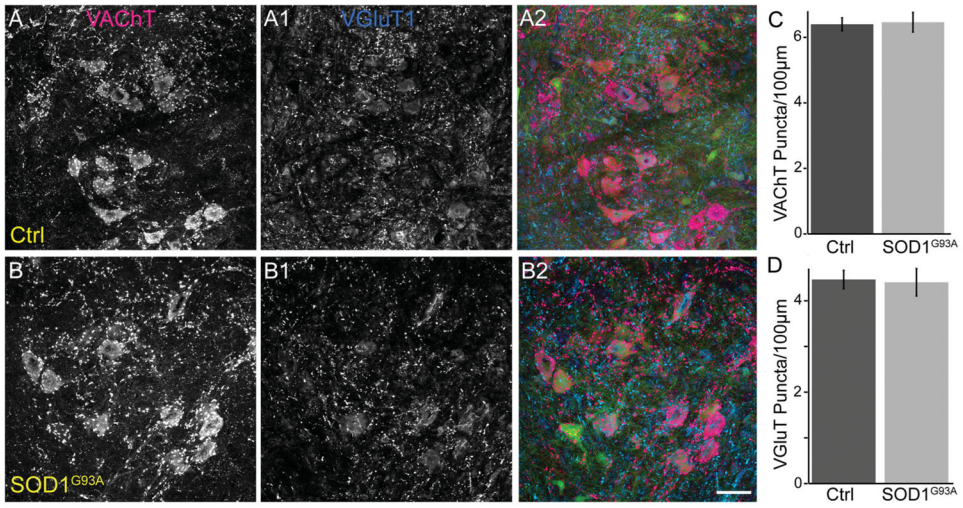

Figure 9.

Numbers of VGluT1- and VAChT-positive synapses are unchanged in the spinal cord of 60-day-old SOD1^{G93A} mice. Spinal cords at lumbar region 1 from male 60-day-old control (**A–A2**) and SOD1^{G93A} (**B–B2**) animals expressing YFP in motor neurons were stained with VAChT (red) and VGluT1 (blue). (**C–D**) The number of VAChT and VGluT1 puncta on α-motor neuron somata is the same between 60-day-old control and SOD1^{G93A} mice. At least three animals were examined per group. Error bar = STE. Scale bar = 20 µm.

TABLE 1

Primary Antibodies Used

Antigen	Immunogen	References	Source, catalog No., lot No.	Host species	RRID	Dilution
Synaptotagmin-2	1–5 day zebrafish embryo	Fox and Sanes, 2007; Cooper and Gillespie, 2011	Zebrafish International Resource Center, catalog No. ZDB-ATB-081002-25	Mouse monoclonal, IgG2a	AB_10013783	1:250
Synaptophysin clone Z66	C-terminus of human synaptophysin	Lai et al., 2008; Harrington et al., 2012	Molecular Probes, catalog No. 80130	Rabbit polyclonal	AB_2315414	1:100
Pan-axonal neurofilament	Nonphosphorylated neurofilament H in homogenized rat brain	Sternberger et al., 1982; Petralia et al., 2011	Covance Research Products, catalog No. SMI-312	Mouse monoclonal, IgG1	AB_2314906	1:1,000
Vesicular acetylcholine transporter (VAChT)	Linear peptide; (CEDDYNYYSRS) corresponding to the C-terminus of rat VAChT	Duplan et al., 2010; Enjin et al., 2010; Wootz et al., 2013	Millipore, catalog No. AB1588, lot No. 2167122	Guniea pig polyclonal	AB_11214110	1:250
Vesicular glutamate transporter (VGluT1)	Strep-tag fusion containing amino acids 456–560 of rat VGluT1	Garbelli et al., 2008; Balaram et al., 2015	Synaptic Systems, catalog No. 135303	Rabbit polyclonal	AB_887876	1:250
NeuN	N-terminus of GST-tagged recombinant protein of cell nuclei purified from mouse brain	Mullen et al., 1992; Scott and Lois, 2007	Millipore, catalog No. MAB377, lot No. 2159655	Mouse monoclonal, IgG1	AB_2298772	1:250